IEEE Access
Multidisciplinary ⋮ Rapid Review ⋮ Open Access Journal

Received December 31, 2019, accepted January 5, 2020, date of publication January 8, 2020, date of current version January 15, 2020.

Digital Object Identifier 10.1109/ACCESS.2020.2964766

Lateral Pipeline Buckling Detection via Demagnetization and Interior Magnetic Measurement

LI JIAN, LI MINGZE, HUANG XINJING, FENG HAO, AND RUI XIAOBO

State Key Laboratory of Precision Measuring Technology and Instruments, Tianjin University, Tianjin 300072, China
Binhai International Advanced Structural Integrity Research Centre, Tianjin 300072, China

Corresponding author: Huang Xinjing (huangxinjing@tju.edu.cn)

This work was supported in part by the National Natural Science Foundation of China under Grant 61773283 and Grant 51604192, and in part by the Project funded by China Postdoctoral Science Foundation under Grant 2018M630271.

ABSTRACT Thermal buckling of subsea pipelines often occurs and seriously threatens pipeline safety. The spherical detector (SD) can realize quasi real-time detection of pipeline buckling owing to its low blockage risk and convenient launch-retrieval deployment. Vertical buckling can be judged by the rolling speed of the SD, while lateral buckling can only be judged by the interior magnetic fields. However, irregular magnetic remanence of the pipeline seriously hinders the magnetic detection of lateral buckling. To against this problem, this paper proposes a method of detecting the lateral pipeline buckling via demagnetization and interior magnetic measurement. It is experimentally demonstrated that demagnetization can remove most of the remanence of the pipeline and make the interior magnetic fields more regular and uniform; After the pipe is demagnetized, both severe and weak lateral bucklings can be sensitively indicated by the single or double peaks of the interior magnetic fields measured by the SD. The interior magnetic fields are also experimentally demonstrated capable of indicating the first and recurring weak buckling through comparing with the previous detection data.

INDEX TERMS Pipeline buckling, detection, spherical detector, magnetic field.

I. INTRODUCTION

Subsea pipeline buckling often occurs due to thermal expansion, because the crude oil transported inside is usually heated to a very high temperature in order to prevent condensation [1]–[6]. When the axial extension increases to a certain extent, an overall vertical or lateral buckling may occur in the form of large deflection and deformation, as shown in Figure 1. When the pipeline is buried shallow, vertical buckling is easy to occur, and when the soil on one side is soft, lateral buckling is easy to occur.

Buckling deformation can accelerate the damage of subsea pipelines. On one hand, it may cause the tensile stress to exceed the ultimate yield strength of the pipe steel, directly resulting in rupture and leakage. On the other hand, the concrete and the protecting coating of the buckled pipe section that has not yet broken will crack or strip, making the steel pipe directly contact with the salty water. The buckled pipe will thus suffer serious stress corrosion. Therefore, it is very significant to periodically, frequently, and timely detect the subsea pipeline buckling.

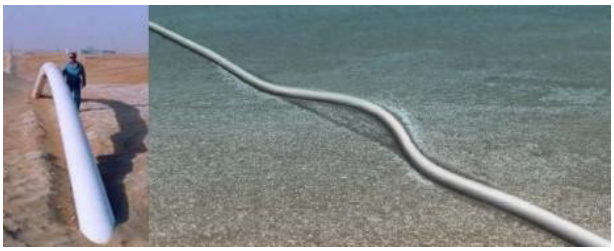

FIGURE 1. Examples of vertical and lateral bucklings of subsea pipelines [4].

Possible methods of pipeline buckling detection can be divided into three categories: exterior methods based on Remotely Operated Vehicles (ROVs) and Autonomous Underwater Vehicles (AUVs), surface attached distributed optic fiber sensor (DOFS), and interior detector. ROVs can approach and clearly observe the pipelines with underwater

The associate editor coordinating the review of this manuscript and approving it for publication was Guijun Li.

cameras and lamps; ROVs requires long-term and real-time supports from the mother-ship through umbilical cable, so the cost is very high but the inspection efficiency is very low. Limited by the umbilical cable length, ROV can only be used in shallow water [7], [8]. AUVs can freely and autonomously swim without the umbilical cable. However, AUVs cannot closely approach the seabed pipelines and can only roughly image the pipeline with sonars at a distance; Resolution is too low to identify the pipeline buckling [9]–[12]. Both ROV and AUV are too costly to be frequently deployed. They are not suitable or competent for subsea pipeline buckling detection.

DOFS based on Brillouin scattering can detect and locate pipeline buckling via remotely monitoring stain changes. Zou for the first time employed a Brillouin DOFS to detect pipe-wall buckling by measuring the longitudinal and hoop strain distributions along the outer surface of the pipeline; The data measured by the Brillouin DOFS is comparable to that by strain gauges [13]–[15]. Zhang C used carbon-coated fibers to identify the pipeline buckling under controlled laboratory conditions; the location and progression sequence of buckling patterns can be successfully predicted by the broadening factor of the Brillouin spectrum width, prior to their visual detection [16]. Zhang S used common conjugate beam method to calculate the pipeline displacement from the strain measured by the Brillouin DOFS [17]. Feng proposed a method of monitoring the upheaval buckling of subsea pipelines by using a new Brillouin DOFS; three sensors with $2\pi/3$ interval were deployed around the circumference of the pipeline to separate the bending- and axial force-induced strains [18]. Feng also mounted the Brillouin DOFS on the outer surface of the pipeline to monitor the longitudinal strains, and then the bending-induced strain is extracted to detect the occurrence and evolution of lateral buckling [19]. However, it is very difficult to adhere a bunch of fragile optic fibers onto the surface of a subsea pipeline, so there are very few subsea pipelines that have optic fiber accompanied.

Traditional cylindrical interior detectors, which are called Pipeline Inspection Gauges (PIGs), measure pipeline trajectory based on inertial navigation system (INS); if a buckling occurs, local mutation of the pipeline trajectory can be seen. Since there is no GPS and above ground marker, INS cannot work for a long distance inside a subsea pipeline and the positioning will shortly diverge and fail. At present, pipeline trajectory measurements based on PIG and INS were only tested on pipelines no more longer than 2km [20]–[23]. INS based method is only applicable by PIGs that have high risk of blockage, but not suitable for the spherical detector (SD) [24]–[26] that has low risk of blockage and is capable of performing quasi real-time detection.

A buckling pipeline is accompanied with changes of both the geometric shape and the interior stress. Due to the magnetomechanical effect that magnetization of ferromagnetic material in ambient magnetic fields can be changed by the stress [27], [28], the magnetization in the pipe wall can be changed by the pipeline buckling stress, and the magnetic field distributions inside the buckled section will present special characteristics, which can be utilized to determine whether there is buckling.

Based on this idea, a method of detecting the buckling of subsea pipelines through demagnetization and interior magnetic measurement is proposed and experimentally demonstrated. First, this paper verifies the equivalence of demagnetization effects from the inside and outside via finite element simulations and demagnetization treatment testing. Second, the method of using the SD to detect the vertical and lateral pipeline bucklings are briefly introduced to present the uniqueness and challenge of lateral buckling detection. Third, experiments are carried out to demonstrate whether demagnetization can make the interior magnetic fields more regular and uniform and remove most of the magnetic remanence in order to obtain high sensitivity. Fourth, magnetic field distributions inside lateral large buckling pipes are thoroughly studied in order to summarize available magnetic characteristics. Finally, the detection ability of weak lateral buckling is demonstrated by ingenious experiments.

II. METHOD

This method consists of two parts: (1) Demagnetize the pipeline to remove the original magnetization, so that the interior magnetic fields become uniform and more sensitive to the deformation and stress changes. Via thorough demagnetization for only once, the interior magnetic fields can maintain regular for a long time, even permanently. It is not necessary to demagnetize the pipeline again for the subsequent buckling detections. The later experiments in this paper also demonstrate this point. (2) The SD featuring convenient and frequently repeatable deployment is employed for quasi real-time detection. Component layout inside the SD will be optimized by this paper to ensure the high quality of test data.

A. DEMAGNETIZATION THEMES

Oil and gas pipelines have severe and irregular original magnetizations, which are also called magnetic remanence. These remanence are generated by the combined action of stress and ambient magnetic fields during the process of production, transportation, welding and laying. The remanence can make the magnetic fields in the pipeline uneven and messy. Figure 2 displays the magnetic fields inside a section of a long field pipeline detected by the SD, where Figure 2 (a) is overall view and Figure 2 (b) is detail view. It can be seen that the interior magnetic field fluctuation is very severe, so the irregular and complicated magnetization is distributed everywhere on a field steel pipeline. For such a pipeline, even if buckling and displacement occur and cause the stress change, the interior magnetic variance controlled by the magnetomechanical effect will be submerged in such strong magnetic background noise and is therefore difficult to identify.

Therefore, in order to achieve a highly sensitive magnetic detection of the lateral pipeline buckling, it is necessary to demagnetize the pipeline. The field pipeline can be demagnetized from the inside by PIGs, because it is difficult to reach a

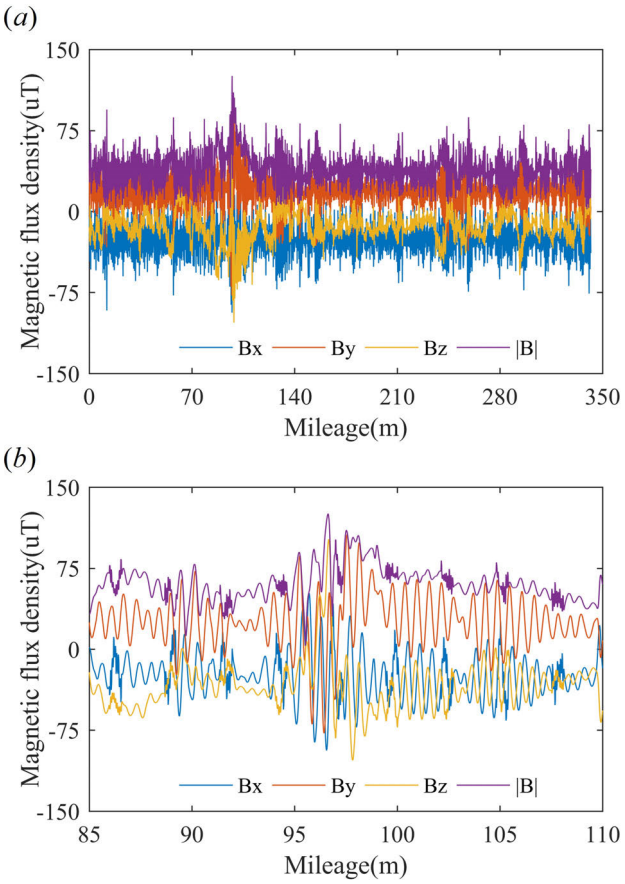

FIGURE 2. Magnetic fields inside a field pipeline are nonuniform and fluctuating due to irregular original magnetizations over a long (a) and short (b) section.

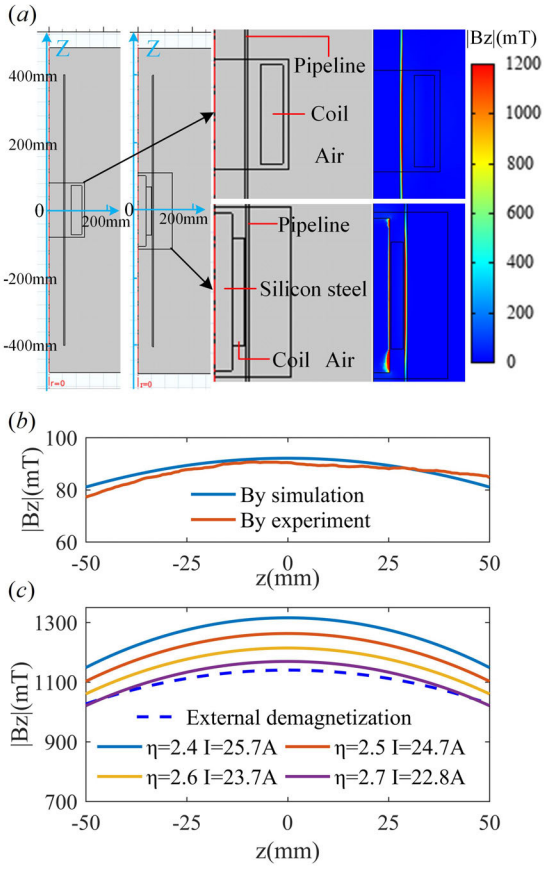

FIGURE 3. Equivalence verification of interior and exterior demagnetizations: (a) Simulation models and results when the demagnetization coil is outside or inside a steel pipe; (b) Experimental verification of exterior demagnetization simulation through comparing |Bz| on the coil axis; (c) Comparison of demagnetization capacities of interior and exterior demagnetizers through comparing |Bz| at the middle of the pipe wall.

buried pipeline from the outside. However, under laboratory conditions, demagnetization is easier to carry out from the outside than inside for an uncovered pipeline. It only needs to coaxially put an alternating current coil on the pipe from the outside, and then move the coil to continuously demagnetize each part of the pipe. It is necessary to prove that the effects of interior and exterior demagnetizations are equivalent, before carrying out exterior magnetization for the study of lateral buckling magnetic detection in lab.

COMSOL, a finite element simulation software, is used to calculate and compare the magnetization ability of the inner and outer coils for the pipeline. As shown in Figure 3 (a), the simulation adopts a 2D axisymmetric model, which is solved in the frequency domain. In the exterior demagnetization model, a steel pipe is trapped by a coil, and all the parameters used in the simulation are the same to those used in the subsequent experiments, so as to experimentally verify the correctness of the simulation results. The inner diameter of the coil is 160mm, the outer diameter is 240mm, the length is 180mm, the number of turns is 726, and the power is 380V AC. In the interior demagnetization model, the coil is wound on a silicon steel and coaxially placed in the pipe. A transformer is connected in series between the coil and the 380V AC power supply to adjust the demagnetization field intensity and observe whether the interior coil can obtain the same demagnetization intensity as the exterior coil.

The results are shown in Figure 3 (b) and (c). First, the simulation results of exterior magnetization were verified by experiments through comparing |Bz| on the coil axis, as shown in Figure 3 (b). Then, the equivalence of the demagnetization effects inside and outside is confirmed by simulations through comparing |Bz| at the middle of the pipe wall, as shown in Figure 3 (c). In the simulation, voltage ratio of the transformer in the interior demagnetizer, η, was swept to adjust the interior demagnetization intensity. It can be seen that |Bz| increases as η decreases, and when η is less than 2.7, the demagnetization intensity by the interior coil exceeds that by the exterior coil. The current of the interior demagnetization coil is within the bearing capacity (~32 A) of a 4mm^2 copper wire according to China national standard. Therefore, these two methods are able to have the equivalent demagnetization effect. For field pipelines, interior demagnetizer can be used, while in laboratorial conditions, exterior demagnetizer can be used.

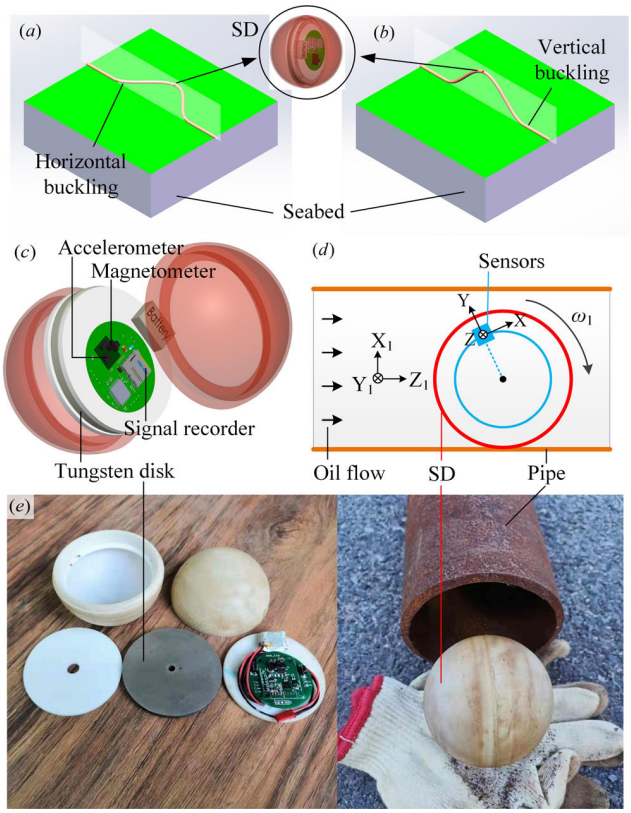

FIGURE 4. Detection schematic of the pipeline buckling by using the SD: (a) Lateral buckling; (b) Vertical buckling; (c) Component layouts inside the SD; (d) The SD is rolling inside a pipe; (e) Prototype of the SD.

B. DEPLOYMENT OF THE SD

The SD is used to measure the magnetic field in the pipeline. Because its diameter is smaller than that of the pipeline, the SD can roll freely forward in the pipeline. The SD has many advantages, such as little possibility of blockage, convenient launch-retrieval operation, frequently repeatable deployment, quasi real-time detection, etc. The schematic of the SD that detects subsea pipeline buckling is shown in Figure 4. A lateral/vertical buckling pipeline is shown in Figure 4 (a)/(b). Component layouts inside the SD is shown in Figure 4 (c). There is a heavy tungsten disk inside the SD, on which the magnetometer and the accelerometer are fixed. As the density of tungsten is 19.35g/cm3, much larger than that of other parts, the tungsten disk can account for 90% of the SD's weight. The tungsten disk is heavy enough to make the SD stably roll around the disk axis. As shown in Figure 4 (d), driven by the fluid in the pipeline, the SD rolls forward around one of its sensor axes, and records the magnetic and acceleration signals. Pipeline vertical or lateral buckling is identified via off-line signal processing after the SD is taken out of the pipe.

In the vertically buckling pipeline, the SD goes through the process of ascending and descending, so its rolling speed will accordingly change. The frequency change of the recorded acceleration can be used to judge whether the pipeline has vertical buckling. However, in the laterally buckling pipeline whose inclination does not vary, the rolling frequency of the SD does not change, so the recorded acceleration cannot be used to identify a lateral buckling. Nevertheless, both the orientation and stress will change when a pipeline buckles, and both can change the interior magnetic fields. Therefore, the interior magnetic characteristics of a pipeline can be used to judge whether a lateral buckling occurs.

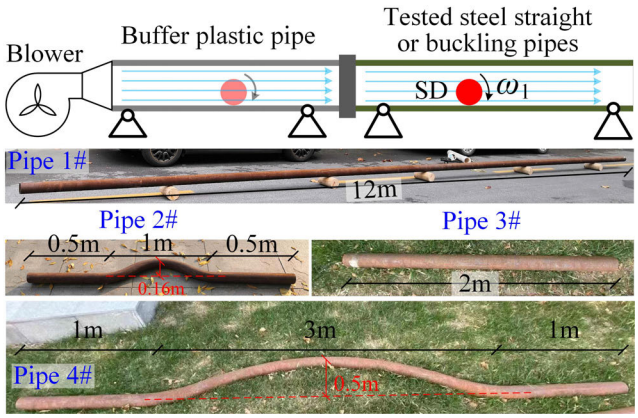

FIGURE 5. Magnetic measurement experiments and tested steel pipes.

Quasi-real time detection of pipeline buckling by the SD is reflected in that the SD can be densely deployed and can be applied to subsea pipelines of any depth. The subsea pipeline buckling may occur and develop every day, every week or every month. The SD can be launched every week or even every day to timely detect pipeline buckling, while the ROVs/AUVs are usually deployed every one or two years. Therefore, the SD's buckling sampling is frequent enough. Unlike the ROVs/AUVs, the SD has an inherent immunity to the harsh external environment like water plants, ocean currents, seabed fluctuations, and is not limited by the depth, because it rolls forward inside the pipeline. Therefore, the SD can inspect all the subsea pipelines while the underwater robots cannot reach too deep pipelines. Cycle counting method is used to calculate the mileage of the SD and the point where buckling occurs.

III. EXPERIMENTS

Several straight and buckling steel pipes were demagnetized by an exterior coil, and the interior magnetic fields were measured by a prototypical SD to verify the benefits of demagnetization and explore the magnetic characteristics of the buckled pipe after demagnetization. Experimental process of using the SD to measure the magnetic fields in the pipe is shown in Figures 5-7. An air pump was used to inject air into the pipe to push the SD to roll forward. The upstream plastic buffer pipe is used to speed up the SD so that the SD can reach a constant rolling speed before entering the steel pipe to be tested. In field application, sticky oil transported by the pipeline can also make the SD stably roll forward and collect high quality magnetic and acceleration signals. There are four steel pipes to be tested with different shapes

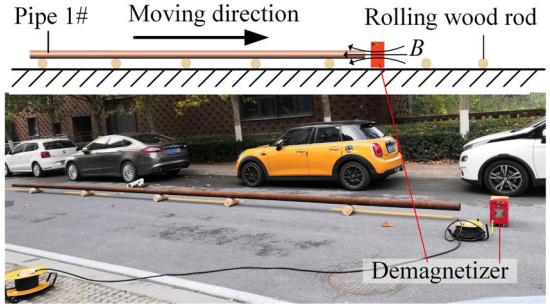

FIGURE 6. Demagnetization experiment.

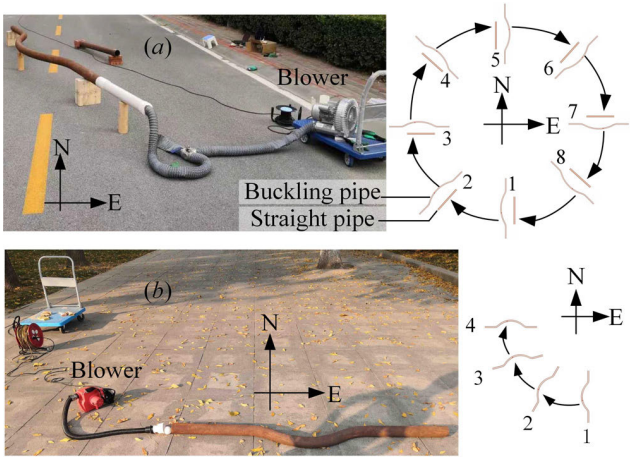

FIGURE 7. Magnetic measurement inside severe buckling pipes with different orientations: (a) large pipe and (b) small pipe.

TABLE 1. Geometric specification of the steel pipes to be tested.

Pipes	Type	L/m	Φ/mm	T/mm	$\overline{\theta}$/°	θ_m/°
1#	Straight, soft	12	114	4	--	--
2#	Buckled	2	80	4	17.74	45
3#	Straight	2	114	5	--	--
4#	Buckled	5	114	5	18.43	60

and lengths, as shown in Figure 5. Pipe 1# is straight, and its size is 114mm×T4mm ×L12m; Pipe 2# is buckled, and its size is Φ80mm×T4mm; Pipe 3# is straight, and its size is Φ114mm×T5mm ×L2m; Pipe 4# is buckled, and its size is Φ114mm×T5mm. The average buckling angles $\overline{\theta}$ of the pipes #2 and #4 are 17.74° and 18.43°, respectively. The max buckling angles θ_m of the pipes #2 and #4 are 45° and 60°, respectively. Three groups of tests were performed by using these pipes.

Experiment 1: Verify the benefits of demagnetization. Interior magnetic fields before and after demagnetization were measured and compared to confirm that demagnetization can make the interior magnetic fields become more regular and uniform and can remove most of the remanence. Among those tested pipes, pipe #1 is much longer than others, so its rigidity is especially low and it may be inevitably and repeatedly stressed during experiment operations. Due to the magnetic mechanical effect, new uncertain magnetization may be generated by the stress and can destroy the thorough demagnetization. Therefore, when the soft long steel pipe was demagnetized, some round woods were placed below the pipe; the demagnetizer was kept still while the pipe was moved through the demagnetizer with a constant speed, as shown in Figure 6. Continuous support by those round woods can protect the pipe from being stressed. The steel pipe that has been demagnetized can be taken as a non-buckling reference pipe.

Experiment 2: Detect severe lateral buckling, as shown in Figure 7. The large pipe 4# was demagnetized with the exterior demagnetizer, and then, as shown in Figure. 7 (a), it was supported by wood rods to make the middle part laterally buckle, and the interior magnetic fields were measured by the SD. As a comparison, the magnetic fields inside the straight pipe #3 after demagnetization were also measured in the same orientation. Considering that the field buckling pipeline can be in any direction, pipes 3# and 4# were rotated clockwise taking the north-south direction as the starting orientation to observe how the magnetic characteristics of the buckling pipe in different directions will change. In order to further verify the correctness and repeatability of the law to be concluded, the same rotation test was carried out on the demagnetized pipe 2#, as shown in Figure 7 (b).

Experiment 3: Detect weak lateral buckling. It is difficult to apply lateral loads to a pipeline to simulate lateral buckling under laboratory conditions, but it is easy to apply vertical loads. ''Vertically loading + rotating'' the long and soft steel pipe 1# was carried out to simulate weak lateral pipeline buckling under laboratory conditions as shown in Figure 8. When the pipe was demagnetized but had not been loaded yet, the interior magnetic fields were measured as a reference without buckling. The pipe was propped up at two ends and applied a vertical load in the middle. After loading, the pipe was laid flat on the ground and the stress is reduced to a very low level. The pipe was rotated around its axis four times with 90° interval to prove that the magnetic field inside is insensitive to the rotation around the pipe axis. In the end, the loading direction was turned to the lateral to test its interior magnetic fields. When the pipe was rotated, the pipe's coordinate system $X_1Y_1Z_1$ was rotated, while the SD's coordinate system XYZ was not rotated. When the rotation angle was 90° or 180°, the direction of the pipe's load became lateral, and the load was equivalent to the lateral buckling load. During the loading, two ends of the pipe were propped up, and upward/downward loads with different extents were applied in the middle to test the sensitivity of the interior magnetic field to the stress.

IV. RESULTS AND DISCUSSIONS

A. DEMAGNETIZATION EFFECTIVENESS

The magnetic fields inside each pipe before and after demagnetization are shown in Figure 9. It can be seen that demagnetization can make the interior magnetic fields more regular

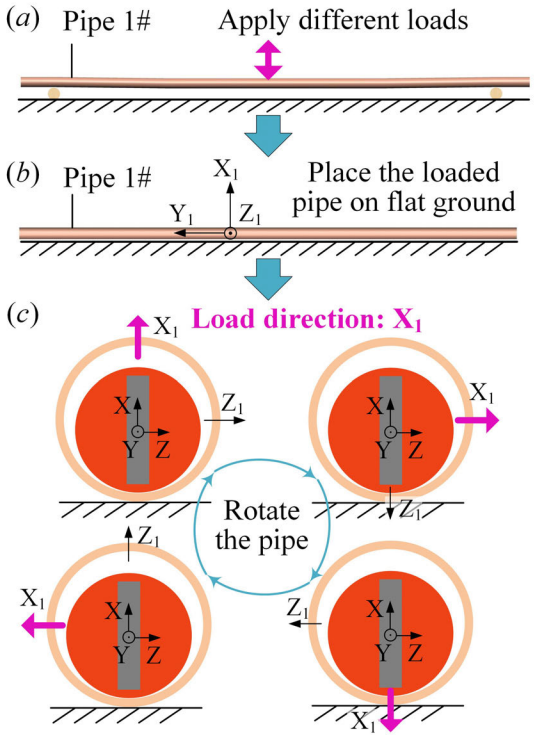

FIGURE 8. Equivalent magnetic measurement inside weak lateral buckling pipe: (a) The pipe is stressed upward or downward with different loads; (b) Place the pipe on the flat ground and release the stress to a very small amount; (c) Rotate the pipe around its axis to make the load direction point to the lateral.

and uniform, and can also remove most of the remanence of the pipes; the background magnetic field in the pipe without information about the buckling can be significantly reduced via demagnetization.

Figure 9(a) displays the magnetic fields inside the pipe 3# before demagnetization, and its amplitude rises from left to right. Figure 9(b) displays the magnetic fields inside the pipe 3# after demagnetization under the same conditions, the amplitude does not go up and is greatly reduced. Figure 9(c) displays the magnetic fields inside the pipe 4# before demagnetization, and the interior magnetic field is very uneven with many noticeable peaks and fluctuations. Figure 9(d) displays the magnetic fields inside the pipe 4# after demagnetization, and the interior magnetic field becomes uniform and the fluctuation is significantly reduced. Figure 9(e) and (f) show the magnetic fields inside the pipe 1# before and after demagnetization. The interior magnetic field becomes more uniform after demagnetization, the fluctuation at the two ends and the middle part is reduced, and the magnetic intensity is also reduced.

Therefore, demagnetization can suppress or even eliminate the irregular background magnetic fluctuations in the pipeline, which is beneficial to utilizing the magnetic field to sensitively identify the existence of weak buckling-caused stress because of the magneto-mechanical effect. It can also be seen from Figure 9 that Bx and By components are very similar, and their envelopes can both almost overlap that

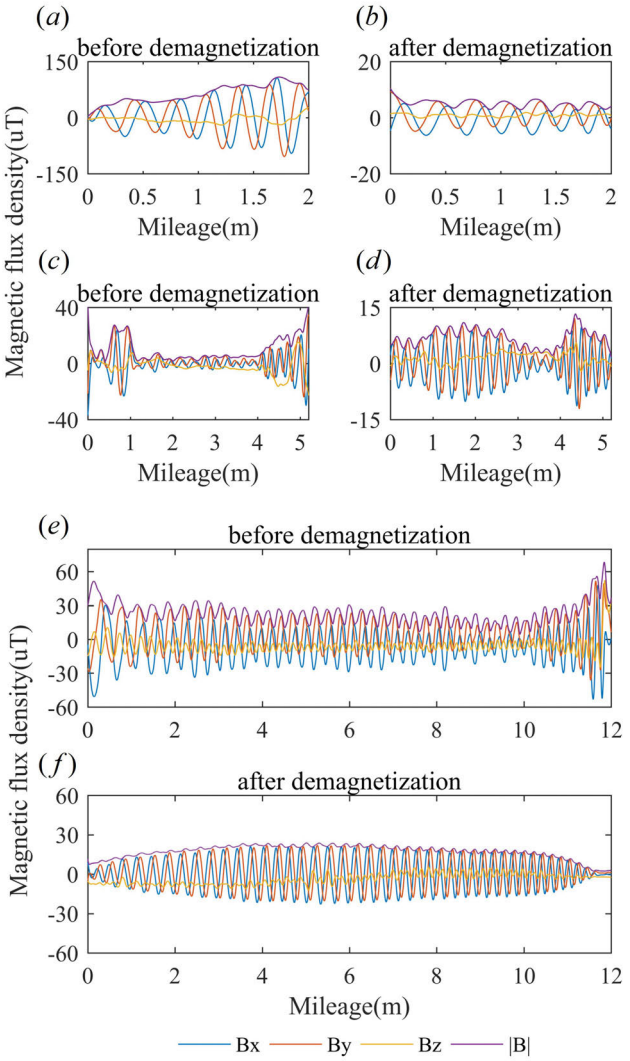

FIGURE 9. Comparisons of magnetic fields inside steel pipes before and after demagnetization: (a) (b), short straight pipe 3#; (c)(d) buckled pipe 4#; (e)(f) long straight pipe 1#.

of |B|; all of the three have the same intensity characteristics. Therefore, in the following discussion, only Bx is used to characterize the magnetic fields inside buckling pipes.

B. DETECTION OF SEVERE LATERAL BUCKLING

The magnetic fields in buckling pipes 4#, 2# and straight pipe 3# after demagnetization in different directions are shown in Figures 10, 11 and 12. It can be seen from Figure 10 that the magnetic fields inside the straight pipe in different directions are uniform and there is no characteristic peak. It can be seen from Figure 11 that for most orientations, the magnetic fields inside the buckling pipe have one or two characteristic peaks, which can clearly indicate the existence of buckling. For a few orientations, the magnetic characteristic peak is not noticeable. The envelope of these characteristic peaks may move, split, or merge as the pipe orientation changes. Although the shape of these characteristic peaks is different, they can be clearly distinguished

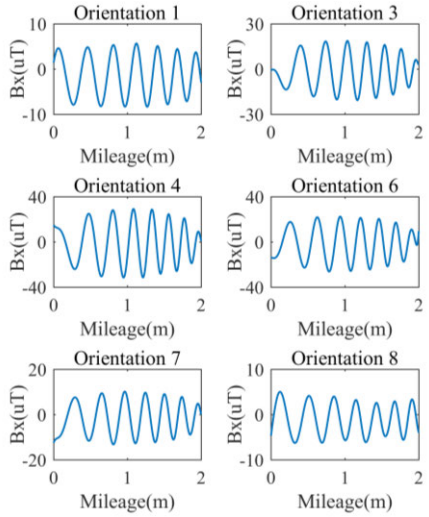

FIGURE 10. Magnetic fields inside the straight steel pipe #3 after demagnetization in different orientations.

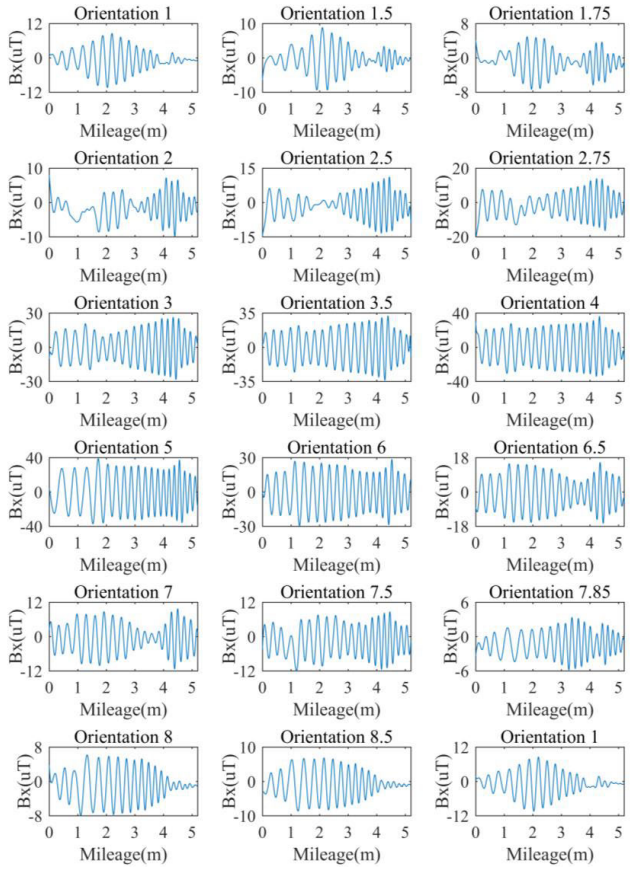

FIGURE 11. Magnetic fields inside the severe buckling large pipe #4 after demagnetization in different orientations.

from that in the straight pipe. In order to verify that the magnetic characteristic peaks in the lateral severe buckling pipe is universal, the magnetic fields inside another severe buckling pipe #2 are measured in different directions, and the results are shown in Figure 12. It is found that the buckling

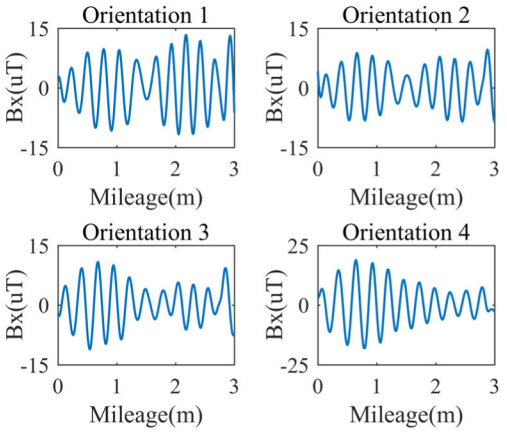

FIGURE 12. Magnetic fields inside the severe buckling small pipe #2 after demagnetization in different orientations.

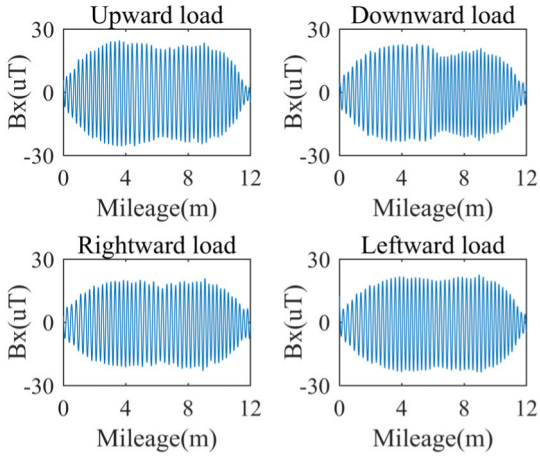

FIGURE 13. Magnetic fields inside a weakly loaded pipe when the load direction points up (a), right (b), down (c), and left (d).

pipe 2# also has distinct magnetic characteristic peaks, and the envelops are very similar to those of the buckling pipe 4#. There are also merging and intensity transfer between the magnetic characteristic peaks for the pipe 2#.

C. DETECTION OF WEAK BUCKLING

When a buckling is very weak, the pipeline may look almost the same to a straight one. However, the stress of the pipe may be changed even if the deformation is very weak. The magnetic fields in the buckling and stressed pipeline will change because of the magnetic-mechanical effect. Since the pipe is axisymmetric, the magnetic field changes due to the buckling stress is independent of the buckling direction and is only related to the extent of the stress. To prove this viewpoint, the experiments shown in Figure 8 were carried out. The pipe 1# was loaded at the middle and then rolled on the flat ground around the pipe axis; the interior magnetic fields were measured and are shown in Figure 13. The magnetic envelopes are almost the same under four equivalent loads in different directions, and have two weak characteristic peaks.

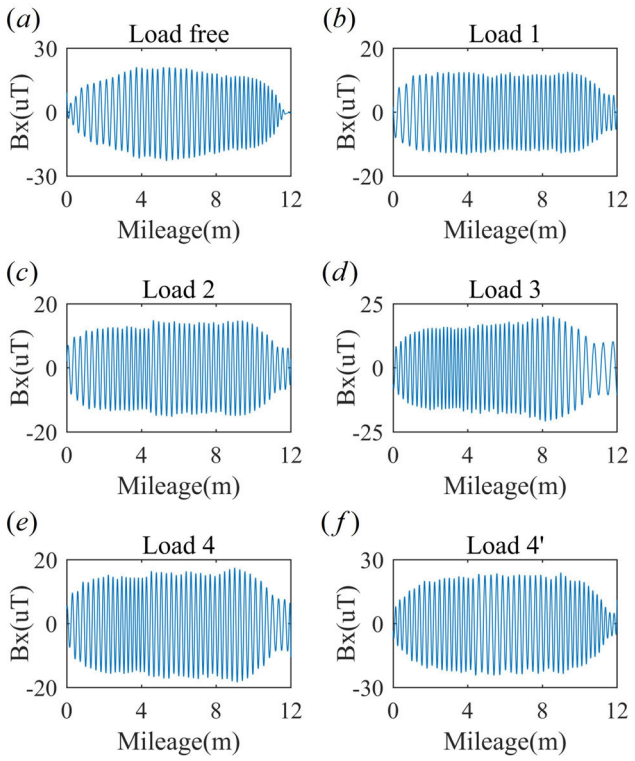

FIGURE 14. Magnetic fields inside a weak buckling pipe with (a) no load, (b)-(e) different levels of loads, and (f) a second load with the same level as (e).

This proves that the magnetic changes caused by the buckling stress is independent of the buckling direction. A vertical buckling pipe can be placed flat on the ground and rotate by 90° to simulate a lateral buckling pipe.

The magnetic fields inside the pipeline are very sensitive to the buckling stress. Due to magnetic hysteresis, even if the stress change has already occurred, the interior magnetic fields can still be rechanged when the stress rechanges. Figure 14 (a) shows the magnetic field inside the pipe 1# after demagnetization when the pipe was laid flat on the ground with no load applied. Figure 14 (b) - (e) shows the magnetic fields inside the pipe 1# when different stresses were applied and the load decreased from Load 1 to Load 4 when the pipe eventually freely sunk. The load difference is about 1-2cm resulted deflection in the middle of the 12m long steel pipe. Figure 14 (f) shows the magnetic fields inside the pipe after it was reloaded, released, and then freely sunk again. It can be seen that the magnetic characteristics inside the pipe under the load are quite different from those inside the straight pipe without load; In the process of changing the load, the magnetic waveform and amplitude also accordingly change. Even if the pipe reverts to its initial load state through a different loading process, the interior magnetic fields are also different due to magnetic hysteresis. Therefore, the magnetic fields inside a pipeline can sensitively indicate the weak buckling, as well as the initial, repeated, and extent-varying stresses caused by various exterior forces. As corrosion may change the component of the subsea pipeline, this method may also be applied to detect pipeline corrosion. Further research can be done toward pipeline corrosion detection in the next work.

V. CONCLUSION

(1) Demagnetization can make the magnetic fields inside the pipeline become more regular and uniform, and can also remove most of the magnetic remanence, which is beneficial to sensitively detect the pipeline stress change and buckling by using the interior magnetic fields.

(2) The demagnetization effects for a steel pipe from the inside and outside are the same; Considering the operability, the field pipeline has to be interiorly demagnetized, while under laboratorial conditions the pipe can be exteriorly demagnetized.

(3) Both severe and weak lateral bucklings can be effectively identified by using the magnetic fields measured by the SD inside the pipeline after demagnetization. The magnetic fields in the severe buckling pipeline have noticeable single peak or double peak characteristics. The magnetic fields in the weak buckling pipeline have weak but still distinguishable characteristic peaks. The interior magnetic fields are demonstrated capable of sensitively indicating the first and recurring weak buckling by comparing with the previous detection data.

REFERENCES

[1] R. W. Shi, "Global buckling of subsea pipelines and pipe-soil interaction," Ph.D. dissertation, Dept. Geotech. Eng., Zhejiang Univ., Zhejiang, China, 2014.

[2] H. Karampour, F. Albermani, and M. Veidt, "Buckle interaction in deep subsea pipelines," *Thin-Walled Struct.*, vol. 72, pp. 113–120, Nov. 2013, doi: 10.1016/j.tws.2013.07.003.

[3] Z. Wang, Y. Tang, and G. Van Der Heijden, "Analytical study of distributed buoyancy sections to control lateral thermal buckling of subsea pipelines," *Mar. Struct.*, vol. 58, pp. 199–222, Mar. 2018, doi: 10.1016/j.marstruc.2017.11.008.

[4] Y. Zhang, Y. M. Xue, X. J. Huang, J. Li, and S. L. Chen, "Characterizations of magnetic field distributions inside buckling pipelines," *Appl. Comput. Electromagn. Soc. J.*, vol. 33, no. 12, pp. 1475–1482, 2018.

[5] H. Karampour, "Effect of proximity of imperfections on buckle interaction in deep subsea pipelines," *Mar. Struct.*, vol. 59, pp. 444–457, May 2018, doi: 10.1016/j.marstruc.2018.02.011.

[6] M. Alrsai and H. Karampour, "Propagation buckling of pipe-in-pipe systems, an experimental study," in *Proc. 12th ISOPE Pacific/Asia Offshore Mech. Symp. Int. Soc. Offshore Polar Eng.*, Oct. 2016.

[7] O. Oskarsson, "Rov based survey: A new, more effective approach," in *Proc. Offshore Technol. Conf.*, Houston, TX, USA, 2016, pp. 3070–3081

[8] C. Mai, S. Pedersen, L. Hansen, K. Jepsen, and Z. Y. Yang, "Modeling and control of industrial ROV's for semi-autonomous subsea maintenance services," *IFAC-PapersOnline*, vol. 50, no. 1, pp. 13686–13691, Jul. 2017, doi: 10.1016/j.ifacol.2017.08.2535.

[9] M. Jacobi and D. Karimanzira, "Multi sensor underwater pipeline tracking with AUVs," in *Proc. OCEANS*, Piscataway, NJ, USA, Sep. 2014, doi: 10.1109/OCEANS.2014.7003013.

[10] H. Xinjing, L. Yibo, D. Fei, and J. Shijiu, "Horizontal path following for underactuated AUV based on dynamic circle guidance," *Robotica*, vol. 35, no. 4, pp. 876–891, Apr. 2017, doi: 10.1017/s0263574715000867.

[11] J. Zhang, Q. Zeng, Z. Zhu, Q. Zhao, J. Yao, and Q. Zhou, "Sonar target recognition research based on AUV," in *Proc. 37th Chin. Control Conf. (CCC)*, Piscataway, NJ, USA, Jul. 2018, pp. 9603–9607, doi: 10.23919/ChiCC.2018.8483330.

[12] J. H. Li, D. G. Park, and H. S. Ki, "Sonar image processing based underwater localization and path planning for AUV's autonomous swimming," in *Proc. 5th Int. Conf. Control, Decis. Inf. Technol. (CoDIT)*, Piscataway, NJ, USA, Apr. 2018, pp. 611–615, doi: 10.1109/CoDIT.2018.8394810.

[13] L. Zou, X. Bao, F. Ravet, and L. Chen, "Distributed Brillouin fiber sensor for detecting pipeline buckling in an energy pipe under internal pressure," *Appl. Opt.*, vol. 45, no. 14, p. 3372, May 2006, doi: 10.1364/ao.45.003372.
[14] L. F. Zhou, X. Y. Bao, F. Ravet, L. Chen, J. Zhou, and T. E. Zimmerman, "Distributed fiber strain sensor based on Brillouin scattering for inspection of pipeline buckling," presented at the 17th Int. Conf. Opt. Fibre Sensors, Beiilingham, WA, USA, 2005.
[15] F. Ravet, L. Zou, X. Bao, L. Chen, R. F. Huang, and H. A. Khoo, "Detection of buckling in steel pipeline and column by the distributed Brillouin sensor," *Opt. Fiber Technol.*, vol. 12, no. 4, pp. 305–311, Oct. 2006, doi: 10.1016/j.yofte.2005.12.002.
[16] C. Zhang, X. Bao, I. F. Ozkan, M. Mohareb, F. Ravet, M. Du, and D. Digiovanni, "Prediction of the pipe buckling by using broadening factor with distributed Brillouin fiber sensors," *Opt. Fiber Technol.*, vol. 14, no. 2, pp. 109–113, Apr. 2008, doi: 10.1016/j.yofte.2007.09.005.
[17] S. Zhang, B. Liu, and J. He, "Pipeline deformation monitoring using distributed fiber optical sensor," *Measurement*, vol. 133, pp. 208–213, Feb. 2019, doi: 10.1016/j.measurement.2018.10.021.
[18] X. Feng, W. Wu, D. Meng, F. Ansari, and J. Zhou, "Distributed monitoring method for upheaval buckling in subsea pipelines with Brillouin optical time-domain analysis sensors," *Adv. Struct. Eng.*, vol. 20, no. 2, pp. 180–190, Feb. 2017, doi: 10.1177/1369433216659990.
[19] X. Feng, W. Wu, X. Li, X. Zhang, and J. Zhou, "Experimental investigations on detecting lateral buckling for subsea pipelines with distributed fiber optic sensors," *Smart Struct. Syst.*, vol. 15, no. 2, pp. 245–258, Feb. 2015, doi: 10.12989/sss.2015.15.2.245.
[20] L. J. Yang, B. Sun, and W. Guo, "Pipeline geographical coordinates Location algorithm based on positioning navigation technology," *J. Shenyang Univ. Technol.*, vol. 36, no. 1, pp. 66–71, 2014, doi: 10.7688/j.issn.1000-1646.2014.01.12.
[21] W. M. F. Al-Masri, M. F. Abdel-Hafez, and M. A. Jaradat, "Inertial navigation system of pipeline inspection gauge," *IEEE Trans. Control Syst. Technol.*, to be published, doi: 10.1109/tcst.2018.2879628.
[22] F. R. Huang, L. Y. Sun, L. S. Guo, Y. Li, and F. Qian, "High-accuracy positioning method based on reverse navigation solution in pipeline detection," *J. Chin. Inertial Technol.*, vol. 26, no. 4, pp. 435–439, 2018, doi: 10.13695/j.cnki.12-1222/o3.2018.04.003.
[23] P. Zhang, C. M. Hancock, L. Lau, G. W. Roberts, and H. De Ligt, "Low-cost IMU and odometer tightly coupled integration with Robust Kalman filter for underground 3-D pipeline mapping," *Measurement*, vol. 137, pp. 454–463, Apr. 2019, doi: 10.1016/j.measurement.2019.01.068.
[24] S. Guo, S. Chen, X. Huang, Y. Zhang, and S. Jin, "CFD and experimental investigations of drag force on spherical leak detector in pipe flows at high Reynolds number," *Comput. Model. Eng. Sci.*, vol. 101, no. 1, pp. 59–80, 2014, doi: 10.1016/j.physd.2014.04.003.
[25] X. Huang, S. Chen, S. Guo, T. Xu, Q. Ma, S. Jin, and G. S. Chirikjian, "A 3D localization approach for subsea pipelines using a spherical detector," *IEEE Sensors J.*, vol. 17, no. 6, pp. 1828–1836, Mar. 2017, doi: 10.1109/jsen.2016.2586998.
[26] G. Lin, Z. Zhoumo, H. Xinjing, L. Jian, and C. Shili, "Vibration detection of spanning subsea pipelines by using a spherical detector," *IEEE Access*, vol. 7, pp. 7001–7010, 2019, doi: 10.1109/access.2018.2890024.
[27] D. C. Jiles, "Theory of the magnetomechanical effect," *J. Phys. D, Appl. Phys.*, vol. 28, no. 8, pp. 1537–1546, 1995.
[28] J. W. Li, "Studies on the magnetomechanical theory and experiment of ferromagnetic materials under weak mechanic field," Ph.D. dissertation, Dept. Gen. Mech. Fundam. Mech., Harbin Inst. Univ., Harbin, China, 2012.

LI JIAN received the B.E., M.E., and Ph.D. degrees from TJU in 1994, 1997, and 2000, respectively. He is currently a Professor with TJU. He also works at the State Key Laboratory of Precision Measuring Technology and Instruments and the Binhai International Advanced Structural Integrity Research Centre, Tianjin University, Tianjin, China. His research interests include pipeline leak detection and pipeline safety warning.

LI MINGZE received the B.S. degree from TJU, in 2018. He is currently pursuing the master's degree with the Instrument Science and Technology Department, Tianjin University. His research topics are related to orientation and localization of pipelines.

HUANG XINJING received the B.S. and Ph.D. degrees from TJU, in 2010 and 2016. He is currently an Assistant Professor at TJU. He also works at the State Key Laboratory of Precision Measuring Technology and Instruments and the Binhai International Advanced Structural Integrity Research Centre, Tianjin University, Tianjin, China. His research interests are structural health monitoring and damage detection for infrastructure.

FENG HAO received the B.E. and Ph.D. degrees from TJU, in 2006 and 2011, respectively. He is currently an Associate Professor with TJU. He also works at the State Key Laboratory of Precision Measuring Technology and Instruments and the Binhai International Advanced Structural Integrity Research Centre, Tianjin University, Tianjin, China. His research interest includes pipeline safety warning.

RUI XIAOBO received the B.S. degree from Tianjin University, in 2014, where he is currently pursuing the Ph.D. degree. His main research interests include piezoelectric energy harvesting and intelligent sensing technology.